https://doi.org/10.5194/egusphere-2025-2757
Preprint. Discussion started: 8 July 2025

Estimating oceanic vertical velocities in a wind-influenced coastal environment

Maxime Arnaud[1], Anne Petrenko[1], Jean-Luc Fuda[1], Caroline Comby[1], Anthony Bosse[1], Yann Ourmières[1], and Stéphanie Barrillon[1]

[1]Aix Marseille Univ., Université de Toulon, CNRS, MIO, 13288, Marseille, France

Correspondence: Maxime Arnaud (maxime.arnaud@mio.osupytheas.fr)

Abstract. Despite the challenge to measure them due to their small intensities, oceanic vertical velocities constitute an essential key in understanding ocean dynamics, ocean-atmosphere and biogeochemistry interactions. Coastal events and fine-scale processes (1-100 km / days to weeks) can lead to high-intensity vertical velocities. Such processes can be observed in the Northwestern Mediterranean Sea. In particular, the Gulf of Lion is a region prone to intense north-westerly and easterly wind episodes, that strongly impact the oceanic circulation. The JULIO mooring (JUdicious Location for Intrusion Observation), located on the boundary of the Eastern side of the Gulf of Lion's shelf at the 100m isobath, provides Eulerian measurements of tridimensional current velocities since 2012. Vertical velocities measured at JULIO are consistent with the ones measured by two other methods: a Free Fall Acoustic Doppler Current Profiler and an innovative Vertical Velocity Profiler. To measure physics-driven vertical velocities, we developed a method to identify and filter out biology-induced vertical velocities. Combining satellite and in situ observations with wind model outputs, we identify wind-induced downwelling and upwelling events at JULIO associated to physics-driven vertical velocities with maximum amplitudes of -465/138 $m\ day^{-1}$. The order of magnitude of w depends on the spatio-temporal scale of its analysis. Hence this multimethod analysis underlines the need for high frequency spatio-temporal measurements in such coastal areas forced by intense wind episodes.

1 Introduction

Regardless of their presence in most ocean dynamic process, vertical velocities (hereafter referred as W) remain one of the most complex aspect of today's oceanography. With intensities usually several orders of magnitude lower than those of horizontal currents, W have been roughly characterized or approximated in the past decades. A breakthrough of (sub)mesoscale resolving models and measurement methods allowed a better understanding of their dynamics and paved the way for studies combining a wide range of methods. These oceanic vertical velocities can play a key role in fine-scale (1-100 km / days to weeks) physical processes, such as (sub)mesoscale fronts, eddies and others, as detailed in Mahadevan and Tandon (2006) using a wind forced upper ocean circulation model. Moreover, it has been shown that submesoscale physics have a definite impact on oceanic phytoplankton distribution and primary production through different fine-scale features: combining glider measurements and altimetry-derived dynamic topography through quasigeostrophic theory, Ruiz et al. (2009) estimated large-scale vertical motions linked to chlorophyll transport in the Alboran Sea. A very complete summary of submesoscale mechanisms, their induced

https://doi.org/10.5194/egusphere-2025-2757
Preprint. Discussion started: 8 July 2025

vertical velocities, and impact on phytoplankton primary production has been carried out by Mahadevan (2016), as well as one on primary export pathways in Siegel et al. (2023).

Various methods have been developed during the last decades to estimate W. The most widely used method for these W measurements features current profilers such as Acoustic Doppler Current Profilers (ADCPs). These ADCPs can be used in different ways, namely mounted on the hull of a vessel or on a mooring line, descended while tied up to a sampling carousel, or mounted on autonomous underwater gliders. In the Gulf of Mexico, D'Asaro et al. (2018) measured $10^{-2}\ m\ s^{-1}$ W using an upward-looking ADCP attached to a neutrally buoyant Lagrangian float following three-dimensional movements of water. The same method used by Tarry et al. (2021) in the Alboran Sea exhibited downward vertical velocities up to $10^{-2}\ m\ s^{-1}$ versus upward vertical velocities of $\approx 10^{-3}\ m\ s^{-1}$. Lowered ADCP observations also allowed Thurnherr (2011) to measure the W of few $10^{-2}\ m\ s^{-1}$ reaching a precision of $\approx\ 5 \times 10^{-3}\ m\ s^{-1}$.

Apart from acoustic measurements, glider measurements allow to estimate W as the differences between the glider vertical velocities (velocities derived from pressure variations) and their theoretical velocities extracted from a flight model. In the Labrador Sea, Frajka-Williams et al. (2011) estimated W values of $9 \times 10^{-3}\ m\ s^{-1}$ in the stratified water column and $2.1 \times 10^{-2}\ m\ s^{-1}$ in the mixed layer using gliders. Frajka-Williams et al. (2011) was able to estimate the measurement error of W from gliders respectively at 5×10^{-3} and $4 \times 10^{-3}\ m\ s^{-1}$. Other 3-months observations in the same area by Clément et al. (2024) with gliders allowed to measure downwelling (upwelling) convective plumes of $-4.6 \times 10^{-2}\ m\ s^{-1}$ ($3.2 \times 10^{-2}\ m\ s^{-1}$).

Several other methods are used for W estimation, featuring in situ observations and theory. Indeed, Argo floats allowed Christensen et al. (2024) to estimate values of W of few $10^{-6}\ m\ s^{-1}$ using the rate of change in temperature due to vertical and horizontal mixing, deducing the isotherm displacements over time. Divergence calculations based on Lagrangian drifters have been carried out since decades. Molinari and Kirwan (1975) first conducted such analyses in the Caribbean Sea computing differential kinematic properties (DKP) of the flow, based on observations of expansion yields inside drifter's clusters. This first method paved the way for multiple studies (Richez, 1998; Righi and Strub, 2001; Spydell et al., 2019) and others. In the Alboran Sea, Tarry et al. (2022) combined it with the continuity equation by making the assumption of null W at the surface. This work highlighted that W could vary, within a four-hour time window, from -1.2×10^{-3} to $0.5 \times 10^{-3}\ m\ s^{-1}$ (respectively -100 and 50 $m\ day^{-1}$). Esposito et al. (2023), using divergence from drifters as well, obtained W with orders of magnitude around $1.2 \times 10^{-3}\ m\ s^{-1}$ (100 $m\ day^{-1}$). Using electro-magnetic APEX floats and satellite observations, Jakes et al. (2024) measured W with an order of magnitude of $10^{-3}\ m\ s^{-1}$ (>100 $m\ day^{-1}$) by sampling a cold filament in the region of the Antarctic Circumpolar Current. They used the same treatment method as Phillips and Bindoff (2014) who obtained, in the same region near Kerguelen, a negative depth-averaged W around $10^{-5}\ m\ s^{-1}$ and an associated standard error $\approx\ 10^{-4}\ m\ s^{-1}$.

A model simulation was used in Garcia-Jove et al. (2022) in Alboran Sea frontal regions, supported by in situ observations such as UCTD casts and glider measurements, reaching values of W with an order of magnitude of $10^{-4}\ m\ s^{-1}$ (55 $m\ day^{-1}$).

Another approach for W estimation relies on the Q-vector version of the ω-equation (Hoskins et al. (1978), adapted by Tintoré et al. (1991); Pollard and Regier (1992)) applied in quasigeostrophic theory. Oceanic vertical velocities are thus expressed through the adiabatic QG ω-equation. The numerical solving of the ω-equation, using three-dimensional maps of density and horizontal velocities (Fiekas et al., 1994; Giordani et al., 2006; Hoskins et al., 1978; Rudnick, 1996), provided W with an order

https://doi.org/10.5194/egusphere-2025-2757
Preprint. Discussion started: 8 July 2025

of magnitude from 10^{-5} to 10^{-4} $m\ s^{-1}$. With the same method, Zhu et al. (2024) obtained W using horizontal currents from a ship mounted ADCP, reaching an order of magnitude of 10^{-3} $m\ s^{-1}$ (170 $m\ day^{-1}$) in the Kuroshio-Oyashio extension region.

Regarding other theory based estimations, Cortés-Morales and Lazar (2024) analyzed Linear Vorticity Balance (LVB) from an eddy-permitting ocean circulation model to estimate W and investigate their inter annual variability on large spatial scales. By integrating the geostrophic component of LVB vertically, and average it over 56 years, they estimated W values with an order of magnitude up to 10^{-5} $m\ s^{-1}$: giving us the orders of magnitude for W at large space and time scales. Alternatively, relationships between surface variables (i.e. horizontal velocities, surface density and derived variables) and inferred vertical velocities have been evaluated through different machine learning models by He and Mahadevan (2024).

Our area of study, the Northwestern Mediterranean Sea, exhibits a large scale cyclonic circulation (Millot, 1999). In the Northwestern basin, the Northern Current (NC) constitutes its Northern branch (Millot and Taupier-Letage, 2005). Originating from the Ligurian Sea, this density current follows the coast with a horizontal speed from 0.4 up to 0.7 $m\ s^{-1}$ in winter, seasonal variability affecting its width, depth, and thus, its flow rate (Petrenko, 2003). The Mediterranean Sea, and in particular the Northwestern basin, is a microtidal environment; therefore, the tidal effects are negligible in this study. With regard to atmospheric forcing, the area is prone to intense wind episodes from two main directions: easterly and north-westerly winds. These forcings have been studied as well as their impact on the oceanic circulation (Guenard et al., 2005; Berta et al., 2018; Barral, 2022). These winds exhibit a strong seasonal variability that affects both their direction and speed. Indeed, models (Lebeaupin Brossier et al., 2013), reanalysis (Soukissian and Sotiriou, 2022) and observations (Ragone et al., 2019) showed that the so-called Mistral wind (Northwestern wind) strengthened (from 15 up to more than 20 $m\ s^{-1}$) during the cold seasons and weakened during warmer ones (from 5 to 10 $m\ s^{-1}$), with rare intensity peaks. Strong Mistral episodes enabled deep convection in winter (Testor et al., 2018), associated with non-negligible W (Bosse et al., 2021; Giordani et al., 2017). The Northwestern basin is also subject to numerous fine-scale processes (d'Ovidio et al., 2010, 2019; Barrier et al., 2016; Declerck et al., 2016).

Wind directions also have a direct impact, via Ekman transport, on water masses moving toward or away from coasts, thus generating, respectively, downwellings or upwellings events (Barrier et al., 2016; Mourre et al., 2022). As tidal effects are negligible (Lamy et al., 1981), these upwellings and downwellings are mainly induced by the occurrence of specific wind events, the presence of coasts and of the NC.

The vertical measurements presented before occurred in both coastal and offshore environments out of our area of study. Indeed, few estimations of vertical velocities have also been obtained in our area. Lowered ADCPs paved the way for a new method adapted by Comby et al. (2022) in the Ligurian Sea. Comby et al. (2022) cross-analyzed different observations using ADCPs, with a classical four-beam ADCP and a new generation five-beam ADCP both lowered on carousels, and implemented a new method with a four-beam ADCP free-fall deployment. These methods allowed for measurements of W about several 10^{-3} $m\ s^{-1}$, with standard deviations of the same order of magnitude.

https://doi.org/10.5194/egusphere-2025-2757
Preprint. Discussion started: 8 July 2025

In the Gulf of Lion, Margirier et al. (2017) studied convective events. They compared glider W measurements to ADCP measurements from the LION mooring line (5° N 43° E). They obtained W of a few $10^{-2}\ m\ s^{-1}$, while the measurement error of W from gliders is evaluated at 5×10^{-3} and $4 \times 10^{-3}\ m\ s^{-1}$ (Merckelbach et al., 2010).

Based on the principle of glider flight model, Fuda et al. (2023) have proposed a new approach to measure W: the Vertical Velocity Profiler (VVP). The VVP allowed vertical velocities measurements with orders of magnitude of a few $10^{-3}\ m\ s^{-1}$ in the region of the North Balearic Front.

In the Ligurian Sea, the ω-equation was calculated from ADCP horizontal velocities and densities derived from a moving vessel profiler, leading to estimated vertical velocities of $10^{-4}\ m\ s^{-1}$ (Rousselet et al., 2019). The same method was used by Tzortzis et al. (2021) in the South Balearic Islands frontal region where W was in the order of a few meters per day.

Generally W have very low intensity. Nonetheless, some W can be strong not due to physics-driven processes, but due to biology-induced processes. Diel vertical migrations (DVM) have been analyzed for decades (Enright and Honegger, 1977; Haney, 1988), highlighting both diurnal and seasonal cycles. Heywood (1996) estimated W of several centimeters per second associated to living scatterers using a vessel mounted ADCP. These migrations have been observed with moored upward-looking ADCPs in different regions: Alboran Sea (van Haren, 2014), Corsica Channel (Guerra et al., 2019) and Norwegian Sea (Cisewski et al., 2021). Cisewski et al. (2021) identified specific oceanic and optical conditions as important drivers for these migrations while Guerra et al. (2019) linked DVM to Chlorophyll-a peaks. van Haren (2014) also showed the direct impact of ocean stratification and internal waves on living scatterers behavior and movements. The patchy form of zooplankton swarms has been mentioned in various studies, including Sourisseau et al. (2008); Tarling et al. (2018) who associated ADCP measured W (moored for Sourisseau et al. (2008) and ship-mounted for Tarling et al. (2018)) with echosounder data. The size of living scatterers also impact the time at which vertical migrations take place and the scatterers moving speed (Gastauer et al., 2022). In the Strait of Gibraltar, a recent study coupling an upward-looking ADCP and an echosounder has highlighted the impact of DVMs on the intensity of horizontal currents (Sammartino et al., 2024).

The aim of this study is to measure W in a coastal environment and study specific events such as upwellings or downwellings. To estimate the reliability of our data, different measurement methods are compared and cross-analysed, giving an insight into our measurement precision. An in-situ ADCP multiyears time serie (JULIO mooring) is completed with other observations such as satellite SSH (Sea Surface Height), SST (Sea Surface Temperature), and in-situ temperature measurements. Within the framework of these observations, a thorough analysis of the intensity and variability of W is conducted using the moored ADCP time series dataset.

Our scientific questions are:

- Is the JULIO moored ADCP a reliable tool to measure physics-induced vertical velocities ?
- How do the measured vertical velocities relate to complementary observations ?
- Can we identify typical coastal dynamical processes ?

The paper is structured as follows. In the Data and Methods section, the ADCP dataset is described, followed by datasets obtained with the Vertical Velocity Profiler and the free-fall ADCP method. The first part of the results section consists in the

https://doi.org/10.5194/egusphere-2025-2757
Preprint. Discussion started: 8 July 2025

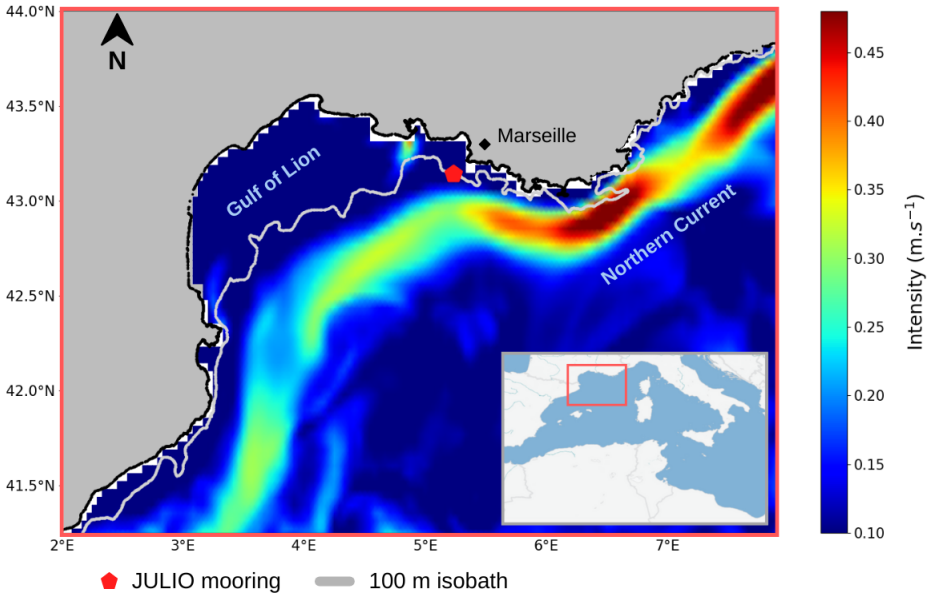

Figure 1. Location of the JULIO ADCP mooring on the averaged December 2022 current horizontal intensity (CMEMS reanalysis)

inter-comparison and validation of W measurements using JULIO ADCP, FF-ADCP and VVP methods. In the second part of the results section, we take a global view of all vertical velocity time series before focusing on a methodology developed to isolate and filter biology-induced signals. This filtering allows to present oceanic dynamics resulting from physical processes in the third part. This latter part outlines the analysis of both physics-induced vertical velocities and surface observations, focusing on two specific cases: upwelling and downwelling events. The outcomes are then discussed in terms of the questions raised on both precision and variability, followed by the conclusions and perspectives.

2 Data and methods

2.1 Moored ADCP (JULIO)

The JULIO (JUdicious Location for Intrusion Observation, Petrenko et al. (2023)) mooring is located offshore Marseille at the border with the Gulf of Lion shelf, on the 100 m isobath (Fig. 1). JULIO is composed of a RDI (Research, Development and Innovation) 300kHz Workhorse Sentinel upward-looking ADCP with four classical beams. Before 2020, it was set up in a bottom anti-trawling device; after 2020 on a short mooring line minimizing the risk of trawling. Moored ADCPs provide tridimensional Eulerian vertical profiles of currents over time, by measuring a shift in frequency between emitted and received sound wave, indicating the velocity of particles suspended in the water, and then transposing these data from a beam reference frame to a geographical one. The method implies the hypothesis that these particles retrodiffusing the acoustic signal are passively drifting in the water, transported by the oceanic currents. The minimum order of magnitude achievable with our

https://doi.org/10.5194/egusphere-2025-2757
Preprint. Discussion started: 8 July 2025

Time serie	First day	Last day	Bin size (m)	ADCP depth (m)
1	02-12-2012	10-23-2012	4	98
2	03-26-2013	03-28-2014	4	98
3	07-17-2014	04-10-2015	4	101
4	12-07-2020	08-31-2021	4	84
5	09-01-2021	06-23-2022	4	82
6	06-24-2022	06-22-2023	2.5	83
7	07-12-2023	05-21-2024	2.5	84

Table 1. JULIO time series with corresponding dates of beginning and ending of data recording, bin size and ADCP depth.

measurements is $1 \times 10^{-3}\ m\ s^{-1}$. Time series are obtained with a time resolution of half an hour and a vertical resolution (i.e. cell size) from 4 m to 2.5 m (Table 1). More informations are available on JULIO's website: https://people.mio.osupytheas.fr/~petrenko/julio.htm.

The observations (interrupted by yearly maintenance and trawling incidents) began in 2012 with an initial purpose: measuring the Northern Current intrusions on the continental shelf of the Gulf of Lion (Barrier et al., 2016). Time series are shown in Table 1.

The 3D current measurements are obtained after a data-quality treatment inherent to the measurement method. A layer, known as the blanking distance, is removed near the ADCP, as a bias is caused by its transducers ringing which ceases progressively with time and thereby influences the closest echoes of the ADCP. The thicknesss of the blanking zone varies between ≈ 5-6 m (varying with slight changes of ADCP configuration throughout the years) from the ADCP depth (Table 1). Another layer, known as the Sidelobe interference layer, is removed at the surface since the water/air interface acts as a powerful reflector, and returns an intense signal to the ADCP. This layer has a thickness of ≈11 m (respectively ≈16-19 m) when the vertical bin size is 2.5 m (respectively 4m). This layer thickness is more conservative than the one calculated as a function of the acoustic beam's slant angle (here 20°), keeping only high-quality data.

The ADCP also provides the strength of the returning ADCP acoustic signal (echo intensity, measured in dB) after hitting particles in the water, which decreases with the distance to the target. At a given distance, the higher the echo intensity, the higher the concentration of particles. We computed the Echo Amplitude Anomaly (EAA) in three steps: 1) we select daytime echo amplitude (between 6AM and 6 PM) to avoid nocturnal phenomena (Sect. 3.3), 2) we compute a trend by applying a rolling mean with a 15 days time window and 3) we subtract this trend from all echo amplitudes, resulting in EAA.

2.2 Vertical Velocity Profiler

The Vertical Velocity Profiler (VVP) is an innovative instrument developed at the MIO laboratory to measure W with the help of a flight model. Based on the methodology developed for the gliders (Merckelbach et al., 2010; Frajka-Williams et al., 2011;

https://doi.org/10.5194/egusphere-2025-2757
Preprint. Discussion started: 8 July 2025

Bosse et al., 2021), W are obtained by comparing the instrument measured velocity (derived from pressure) to its theoretical velocity (obtained with a flight model). The VVP, driven by a propeller to a set depth, rises freely under the sole effect of its positive buoyancy. During the rise, the pressure is measured at 2Hz, giving the instrument vertical velocity through the water column by calculating the pressure time derivative. This velocity is then compared to the theoretical one based on its flight model. Any difference between these values is considered as upward or downward W (Fuda et al., 2023). The VVP allows autonomous measurements of vertical velocities inside the water column with a sampling frequency of 2 Hz and a vertical resolution depending on the rising speed of the VVP. In our case, the rising speed was $7.40 \times 10^{-2} m\ s^{-1}$. As the VVP's wake induces an interfering $20\ s$ period sine wave component on the W of the VVP, the signal is smoothed at a $30\ s$ temporal resolution (the signal is low-pass filtered with a cutoff frequency of $\frac{1}{30}\ Hz$). The VVP profile depth range was from 78.9 to 3 m depth. For this study, we focused on the only VVP rise concomitant with Free-Fall ADCP measurements: on the 06-24-2022 from 9:17 to 9:34 UTC. This time subset matches the reinstallation of the mooring line after data recovery at the JULIO point, since the VVP has been deployed $\approx$ 15 minutes after JULIO was released back into the water.

2.3 Free-Fall ADCP

The Free-Fall ADCP (FF-ADCP) consists of a downward-looking ADCP mounted on a weighted cage, connected to the boat by a rope which is left loose enough on the descent in order to let the ADCP drop free of the ship's movements. This assures a descent of the FF-ADCP as vertical and smoothly as possible. The cage is then pulled back in order to proceed as quickly as possible to the next descent to measure the temporal variability of vertical velocities at the highest possible frequency. With a descent down to 200m at a speed of 0.65 $m\ s^{-1}$, 8 casts can be performed in one hour. Only the top-down profiles are exploited for W measurement, as the pull up carried out with the ship's which introduces large perturbations of the measurement. The work conducted by Comby et al. (2022) presents different data processing methodologies depending on the type of ADCP data used (W from four beams or fifth beam). The main paper recommendation was the use of the free-fall method with a five-beam ADCP which would most likely provide the best W measurement. In our case, with a new fifth beam ADCP, we follow the data treatment of Comby et al. (2022). Namely, 1) the application of three quality criteria 2) the generalization of attitude angles (i.e. pitch, roll and heading) in spherical convention, and a correction of the fifth beam deviation with rotation matrices 3) the removal of the instrument falling speed to the absolute velocity measured and, finally, 4) the 10 seconds temporal smoothing. FF-ADCP data were collected on the same day as both the beginning of the JULIO ADCP 6th time serie and the VVP measurements.

2.4 Wind model

In addition to these in situ observations, model outputs were used. From the global numerical prediction model ARPEGE (Bouyssel et al., 2022), we extracted the horizontal components of wind velocities at 10 meters above the surface, with a horizontal resolution of 0.1°. The model has a temporal resolution of 3 hours. We focused our data analysis at JULIO coordinates (i.e. 43.142° N - 5.233° E), and have expanded our study area to the whole Gulf of Lion's frame (2° E : 7° E ; 41.25° N : 44° N) to discriminate (spatially and temporally) isolated punctual wind peaks from wind episodes that affect the entire region.

https://doi.org/10.5194/egusphere-2025-2757
Preprint. Discussion started: 8 July 2025

2.5 Satellite data

Satellite observations are also analyzed in order to obtain surface data at or surrounding the JULIO mooring.

2.5.1 Sea Surface Temperature

Sea Surface Temperature (SST) product, obtained from Copernicus Marine Services, combines in situ data from Canadian integrated science data management centre (ISDM) and MyOcean In Situ Thematic Centre, with satellite data from MODIS, AATSR, AVHRR, and SEVIRI (Buongiorno Nardelli et al., 2013, 2015). The resulting dataset thus provides daily gap-free observations and a horizontal resolution of $1/16^{th}$ degree. (Mediterranean Sea High Resolution and Ultra High Resolution Sea Surface Temperature Analysis L4 NRT from satellite observations. E.U. Copernicus Marine Service Information (CMEMS). Marine Data Store (MDS). DOI: 10.48670/moi-00172; accessed on 03-03-2025).

2.5.2 Sea Surface Height

Sea Surface Height above sea level (hereafter called SLA for Sea Level Anomaly) dataset gathers observations from SSALTO and DUACS altimetry products, resulting a daily gridded dataset featuring a horizontal resolution of $1/8^{th}$ degree. (European Seas Gridded L4 Sea Surface Heights And Derived Variables Reprocessed (1993 ongoing) from satellite observations. E.U. Copernicus Marine Service Information (CMEMS). Marine Data Store (MDS). DOI: 10.48670/moi-00141; accessed on 03-03-2025).

2.6 In situ Sea Surface Temperature with HTMNet

SST was also measured at 5 coastal stations around JULIO: Carro, Redonne, Cassis, La Ciotat and Le Brusc, located between 5 and 6 degrees of longitude East as part of the HTMNet program (Rey et al., 2020). The temperature is measured since 2019 at the very surface of the water (in the first meter of depth) with a temporal resolution of 2 minutes (HTMNet website: https://htmnet.mio.osupytheas.fr/HTMNET/squel.php?content=accueil.php).

3 Results

3.1 Inter-comparison of W measurements

Three W measurements have been made simultaneously in space and time at the JULIO site in 2022: JULIO's mooring ADCP, VVP, and FF-ADCP (Fig. 2). Note that only in this case and to compare our data properly, JULIO profiles have been vertically smoothed (using a rolling mean), to a vertical resolution of 5 meters. All methods show profiles with values varying mainly between $\pm 1 \times 10^{-2} m\ s^{-1}$ and mean values not significantly different from 0 (2×10^{-4}, 0.0×10^{-3} and -2×10^{-4} $m\ s^{-1}$, respectively for JULIO, VVP and FF-ADCP). In terms of standard deviation, the VVP shows the largest variability with a standard deviation of $\pm 5.9 \times 10^{-3} m\ s^{-1}$ versus the FF-ADCP with $\pm 4.1 \times 10^{-3} m\ s^{-1}$ followed by JULIO ADCP $\pm 1.0 \times 10^{-3} m\ s^{-1}$. These W are observed under calm conditions (South-South-Westerly wind under $10\ m\ s^{-1}$ during the

https://doi.org/10.5194/egusphere-2025-2757
Preprint. Discussion started: 8 July 2025

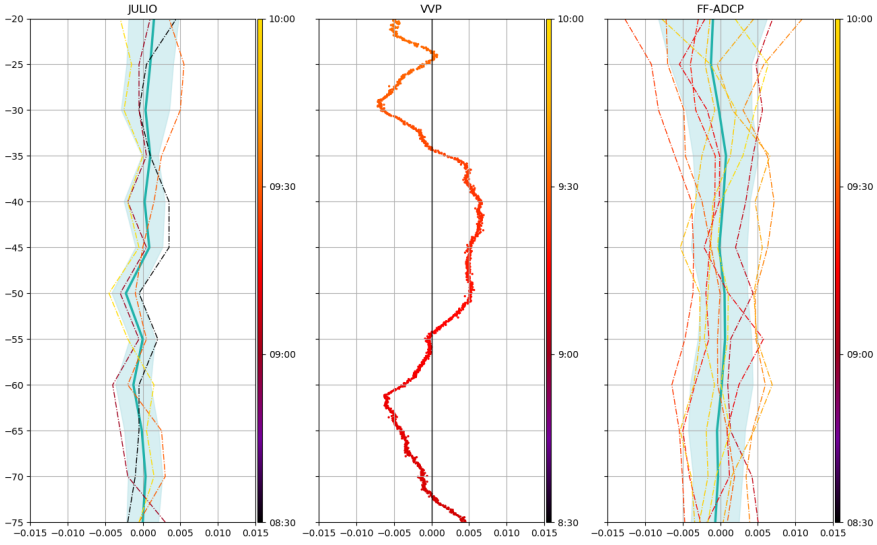

Figure 2. W profiles ($m\ s^{-1}$) as a function of depth. From left to right: JULIO, VVP, and FF-ADCP. In blue, mean (solid line) and standard deviation of the profiles. The profiles are colored-mapped as a function of time (June 24th 2022).

previous 24 hours). All the measurements are compatible, taking into account measurement errors of a few $10^{-3}\ m\ s^{-1}$ and their different intrinsic temporal features: a single FF-ADCP profile lasts 2 to 3 minutes, immediately followed by the next one, the JULIO ADCP measures one instantaneous profile each 30 min, and the VVP profile lasts 17 minutes.

3.2 Vertical velocities on a yearly scale

All measured vertical velocities, through all time series and at all depths, are represented as yearly probability density functions (PDF) with a kernel smoother (Fig. 3). These PDFs exhibit, for all cases except 2013, a negative skewness with a mean consistently below the median value which is equal to zero for all years except 2021 and 2022. Indeed, boxplots highlight that 50% of the values are between -5 and $5 \times 10^{-3} m\ s^{-1}$ as our number of observations for each year remains between 1.7×10^4 and 3.98×10^5.

3.3 Negative vertical velocities at night-time

The signal obtained after the first treatment of ADCP data exhibits an intense and recurring pattern of negative W at night (exemple shown in Fig. 4), at the origin of the negative skewness observed in the general PDFs, with the following characteristics:

- Strong negative vertical velocities appear in patches (with averaged W in the patches $= -1.8 \times 10^{-2}\ m\ s^{-1}$).
- These patches appear with a diurnal cycle spanning ≈8 hours and centered at midnight.
- Those patches are located mainly under the surface (between the surface and ≈50 meters depth).

https://doi.org/10.5194/egusphere-2025-2757
Preprint. Discussion started: 8 July 2025

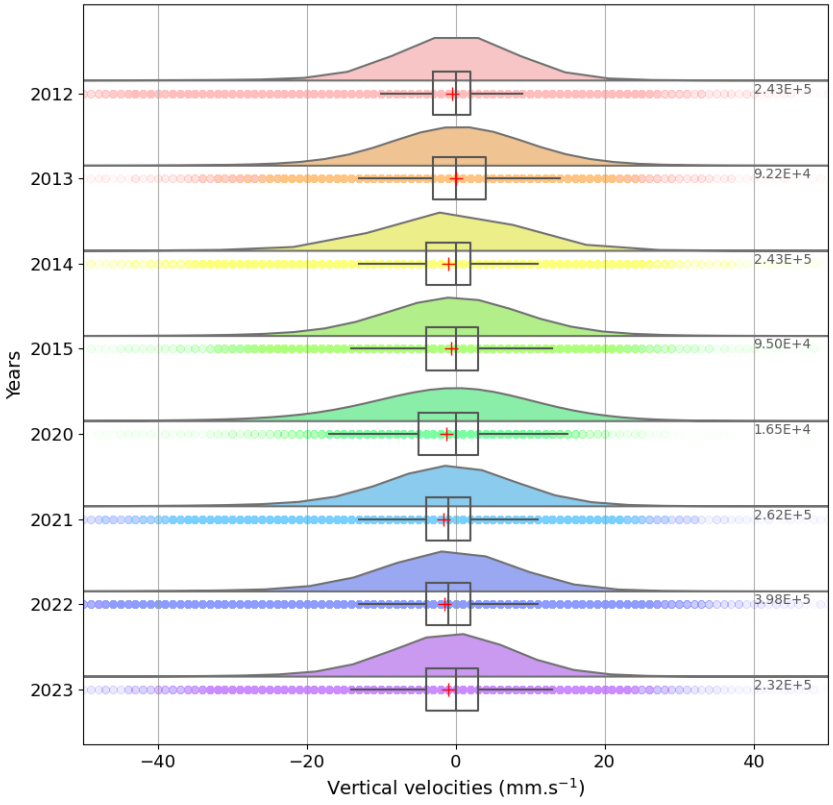

Figure 3. Kernel density estimations of vertical velocities at all depths by year of observation. Scatters: overlapping raw vertical velocity values. Boxplot: whiskers represent extreme values while boxes show the first and third quartiles, thus containing the middle 50% of the values. The black line inside the box represents the median and the red cross, the mean. The number of observations for each year can be found on the right.

– They show a seasonal variability and appear mostly during spring (Fig. 5).

With these characteristics, our assumption is that the origin of this signal is biological. Moreover, despite different spatial scales and species, measurements of diel vertical migrations velocities in the Northeast Atlantic ((Heywood, 1996)) exhibit values with the same order of magnitude: between 2 and $6 \times 10^{-2}\ m\ s^{-1}$. We use the EAA, derived from the measured echo intensity, to help the identification of these patches (Fig.6 top panel). This conjunction of high intensity patches helps to strengthen the biological signal hypothesis.

https://doi.org/10.5194/egusphere-2025-2757
Preprint. Discussion started: 8 July 2025

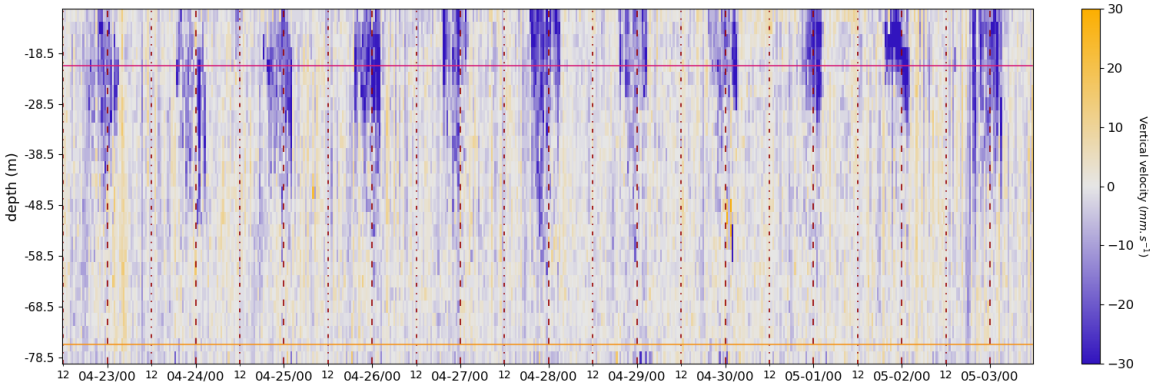

Figure 4. Vertical velocities as a function of depth and time (month-day/hour) over 11 days (April to May 2023). Pink and orange lines show the 19.5 and 75.5 m depth, respectively. The vertical red solid lines mark midnight while the dashed ones mark noon.

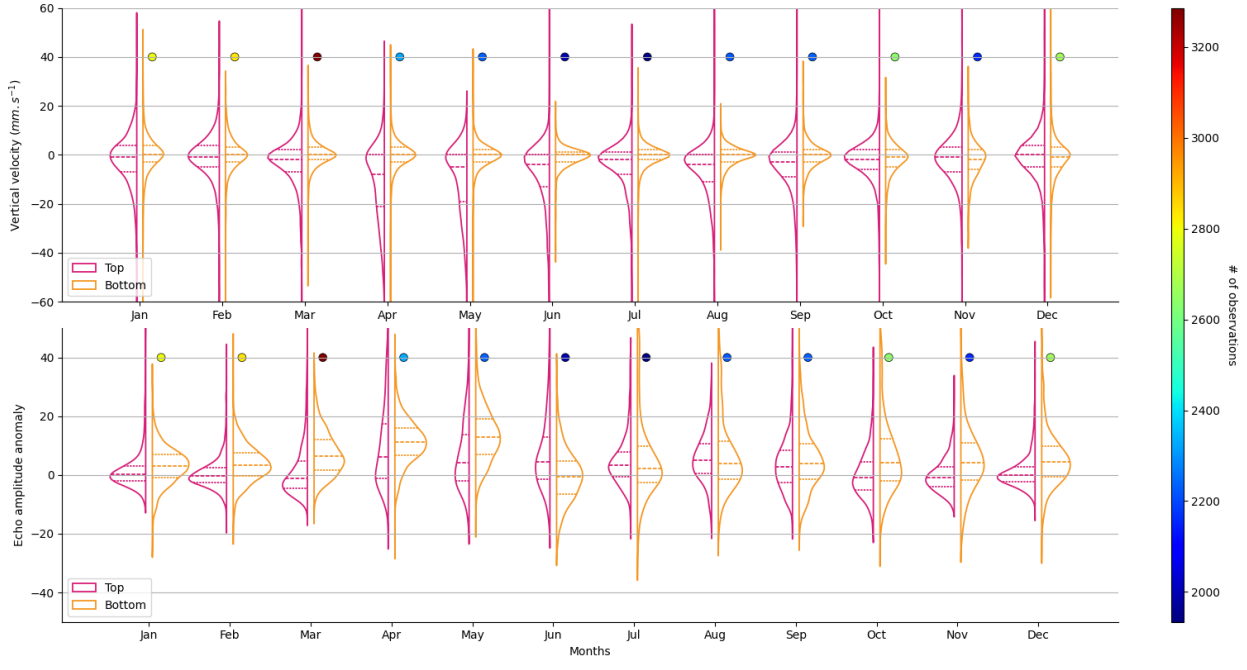

Figure 5. Monthly Probality Density Functions for all the time series, during night time (from 8PM to 4 AM), at shallow and bottom depths (respectively 20 and 75 m; the two different layers referring to the pink and orange lines of Fig. 5). Top : vertical velocities. Down: Echo amplitude anomaly. The colored dots show the number of observations (top and bottom together).

3.4 Patches identification

As targeted patches are characterized by intense W and EAA, their identification relies on thresholds set on both variables. In Fig. 5, we identified negative skewness of W PDF during spring and summer nights in the upper layer, beginning between

https://doi.org/10.5194/egusphere-2025-2757
Preprint. Discussion started: 8 July 2025

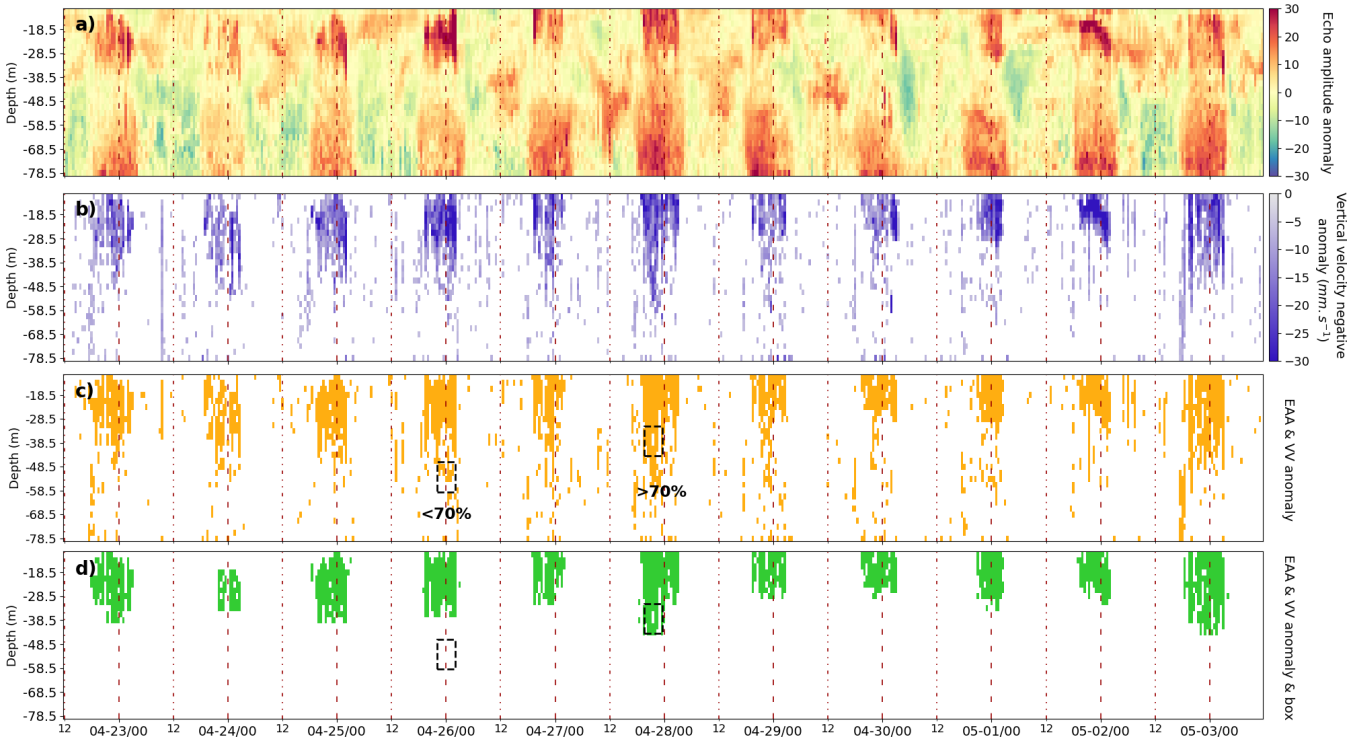

Figure 6. Top to bottom. Echo amplitude anomaly (EAA) as a function of depth and time (month-day/hour) over 11 days (a). Vertical velocities with intensities lower than $-5.0 \times 10^{-3}\ m\ s^{-1}$ (b). Tagged data with $W < -5.0 \times 10^{-3}\ m\ s^{-1}$& $EAA > 0$ (c), black boxes represent the patch criterion. Patches identified as biological signal (d).

March and April, with medians between -2.0 to $-8.0 \times 10^{-3}\ m\ s^{-1}$. The W threshold is set to the middle value :$-5.0 \times 10^{-3}\ m\ s^{-1}$. The top-layer EAA features a strong positive skewness that perfectly matches our W negative anomaly. We therefore consider the combination of W below the threshold of $-5.0 \times 10^{-3}\ m\ s^{-1}$ and EAA above 0, as the initial step to identify biology-induced signal.

A study in Scotia Sea (Tarling et al., 2009) exhibited different types of swarm and their associated characteristics. Their thicknesses can vary from 2 to ≈30 meters, the latter value corresponding to super swarms described as relatively rare in the study. The study also highlights that these phenomena last ≈8 hours. Therefore, we chose to create a virtual box with dimensions of ≈ 15 meters depth and 4 hours long. The method consists in moving the box through the entire dataset over time and depth as shown in Fig. 6 penultimate panel. Inside each position of the box, data are tagged if more than 70% pass both W and EAA thresholds. The tagged data are shown in Fig. 6 d) and thereafter called biological signal. These tagged data are then filtered out of the W, resulting in the physics-driven W, shown in Fig.7.

https://doi.org/10.5194/egusphere-2025-2757
Preprint. Discussion started: 8 July 2025

3.5 Resulting vertical velocities

East of the Gulf of Lion, the main wind forcings are: north-westerly (Mistral) and easterly winds; inducing important cross-shelf water transports, offshore (towards the coast) causing upwellings (downwellings). We consider these winds to be intense when their intensities are above 15 $m\ s^{-1}$. In this section, we focus on these wind episodes, when they occur simultaneously with observations of strong negative (respectively positive) W, lasting at least 4 hours and interpreted as downwelling (respectively upwelling) events. These observations are completed with surface satellite observations.

3.5.1 Upwellings

An upwelling (U_{2022}) with intense positive W was detected at JULIO, after biology filtering, from April 1st to April 3rd 2022 (Fig. 7, right panel). W averaged over depth and time during these two days has a positive value of $1.6 \times 10^{-3}\ m\ s^{-1}$ (versus $-3.9 \times 10^{-3}\ m\ s^{-1}$ before biology filtering) which amounts to ≈138 $m\ day^{-1}$. The horizontal velocity components correspond to a current heading offshore for the entire water column. Such flow matches an intense north-westerly wind episode with speeds exceeding 20 $m\ s^{-1}$ (Fig. 7).

Considering satellite observations, analysed SST (Fig. 7) shows a drop of temperature between April 1st and April 3rd before a general increase according to seasonal trends. The SST decreases from 13.65°C on April 1st, to 12.75°C on April 3rd (0.9°C drop). Over a two-month period (Fig.8), in situ temperature data show a singular temperature drop (2°C) matching the most intense north-westerly wind episode.

Another upwelling (U_{2012}) occurred 10 years before, in March 2012 (Fig. 7, left panel). Though the configuration differs by the absence of biology-induced patches, the same features are observed: strong north-westerly wind, south-eastward current and a steep change in W intensity. The wind episode was just slightly shorter than during the upwelling previously discussed. The W signal varies during this mainly positive period, with a variability decrease as wind intensity drops below 15 $m\ s^{-1}$, which appears to be a common threshold in these two events. The intense positive W during the upwelling lasts from March 5th to March 7th. The depth-time averaged W, $< \overline{W}_{2012} >$, during this period is $1.0 \times 10^{-3}\ m\ s^{-1}$, leading to ≈86 $m\ day^{-1}$. Observations of SST show a small decrease ≈0.5°C leading to a value which remains constant (12.8°C) for two days. Note that U_{2012} happened before HTMNet SST observations were available.

3.5.2 Downwellings

An intense (around 15 $m\ s^{-1}$) easterly wind episode occurred during almost 2 days at the end of fall 2014 (Fig. 9, left panel). This event is followed by a shift in the wind direction and a decrease in its intensity, leading to a weak southerly wind. During this decrease, strong positive meridional component of velocity reflects an onshore horizontal current, leading to a downwelling (D_{2014}). The latter features strong negative W with a depth-time average during the event (12 hours) of $-5.4 \times 10^{-3}\ m\ s^{-1}$ which is equivalent to ≈-465 $m\ day^{-1}$. Surface observations of SLA (Fig. 9) show an increase during November, possibly linked to these easterly winds.

https://doi.org/10.5194/egusphere-2025-2757
Preprint. Discussion started: 8 July 2025

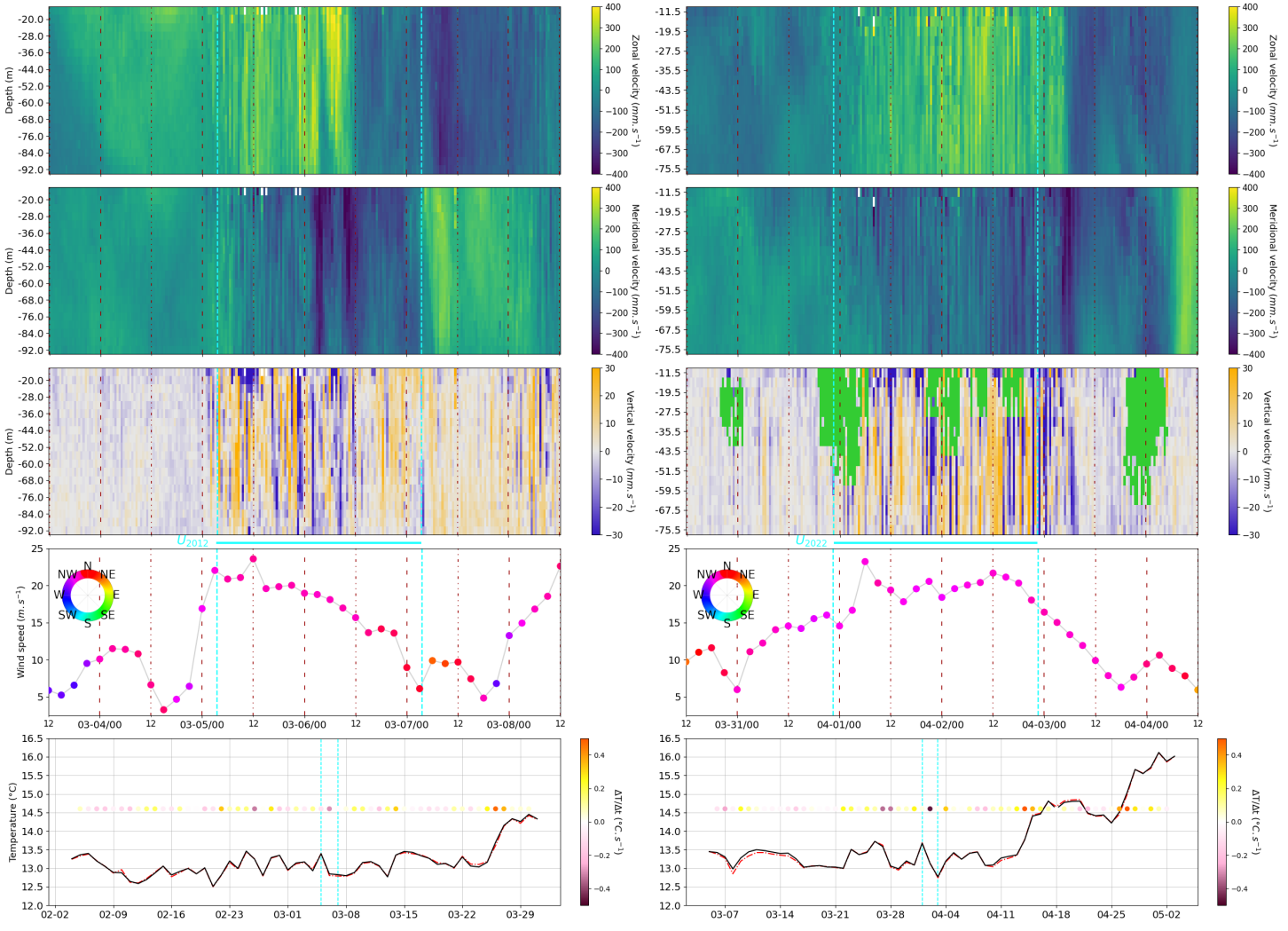

Figure 7. Top to bottom (4 panels): zonal velocity (U) , meridional velocity (V), vertical velocity (W), as a function of depth and time (month-day/hour), wind intensity and direction; all during a 5 days window. Last panel: SST observations over 2 months (month-day) at JULIO (dashed red line for JULIO nearest SST point, solid black line for an average on $\Delta lat = 0.14$ and $\Delta lon = 0.18$ centered on this point), and SST temporal gradient (colored dots). The left and right panels show the two different upwellings: U_{2012} (left) and U_{2022} (right), each indicated between the two vertical cyan lines.

A second downwelling (D_{2021}) taking place in December 2021 also exhibits negative W (Fig. 9, right panel) following a 24 days long easterly wind episode. Horizontal currents show a strong variability during and after the wind episode. The time-depth averaged W during the event (12 hours) indicates a value of $-3.9 \times 10^{-3} m\ s^{-1}$, equivalent to -346 $m\ day^{-1}$. At the same time, SLA is reaching a local maximum after a one week rise (amplitude $\Delta h \approx +0.05m$).

https://doi.org/10.5194/egusphere-2025-2757
Preprint. Discussion started: 8 July 2025

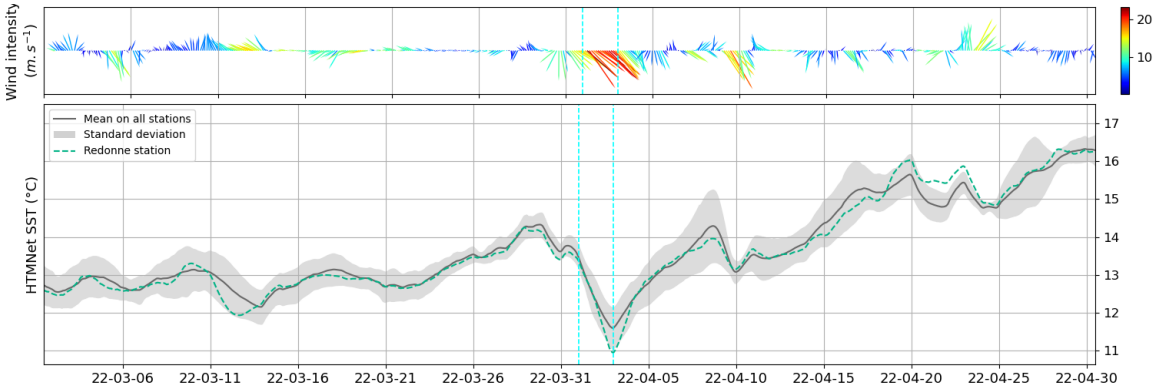

Figure 8. Top to bottom (2 panels): model wind direction and intensity in $m\ s^{-1}$ as a function of time (year-month-day), temperature measured at HTMNet stations in °C for all stations (black line mean value and grey standard deviation) and at the nearest station to JULIO (green). U_{2022} is indicated in both panels between the two vertical cyan lines.

3.6 Overview of W time series

The W global view over all available JULIO time series (Fig. 10) shows a general variability between $\pm 5.0 \times 10^{-3} m\ s^{-1}$. The tagged biological signals show a seasonal pattern: they occur intensely from April to June, and generally extend from March to October with more moderate intensities. Noticeable events such as upwellings and downwellings are visible outside the general variability $\pm 5.0 \times 10^{-3} m\ s^{-1}$. The selected upwellings and downwellings described in this paper were chosen after a global analysis of all the different datasets, as the most intense and coherent events. It should be noted that the targeted upwellings occurred around the beginning of spring and downwellings around the first part of winter.

4 Discussion

On the one hand, the occurrences and intensity of biology-induced intense W highlight the importance of their filtering to obtain physical vertical velocities. On the other hand, studies with different objectives could on the contrary focus on these events in order to study, with the appropriate associated biological measurements, these particles or biological signals.

It is the case in Guerra et al. (2019), where zooplankton diel vertical migrations (DVMs) were identified by matching mean volume backscatter strength and strong vertical velocities in upper layers, combined with zooplankton net samples. However, our biological signal differs from DVMs as the latter includes two phases: an ascent and a descent, leading us to expect respectively positive and negative vertical velocities. Yet at JULIO, we do not observe strictly speaking DVMs but instead we observe negative W patches between dusk and dawn. Some hypotheses are that these patches could be the sign of a sinking phenomena due to satiation of living scatterers that occurs during the night as mentioned in Tarling and Thorpe (2017) or that the angle of displacement of living scatterers could impact the returning signal of the ADCP (pers. comm. M. Ohman).

https://doi.org/10.5194/egusphere-2025-2757
Preprint. Discussion started: 8 July 2025

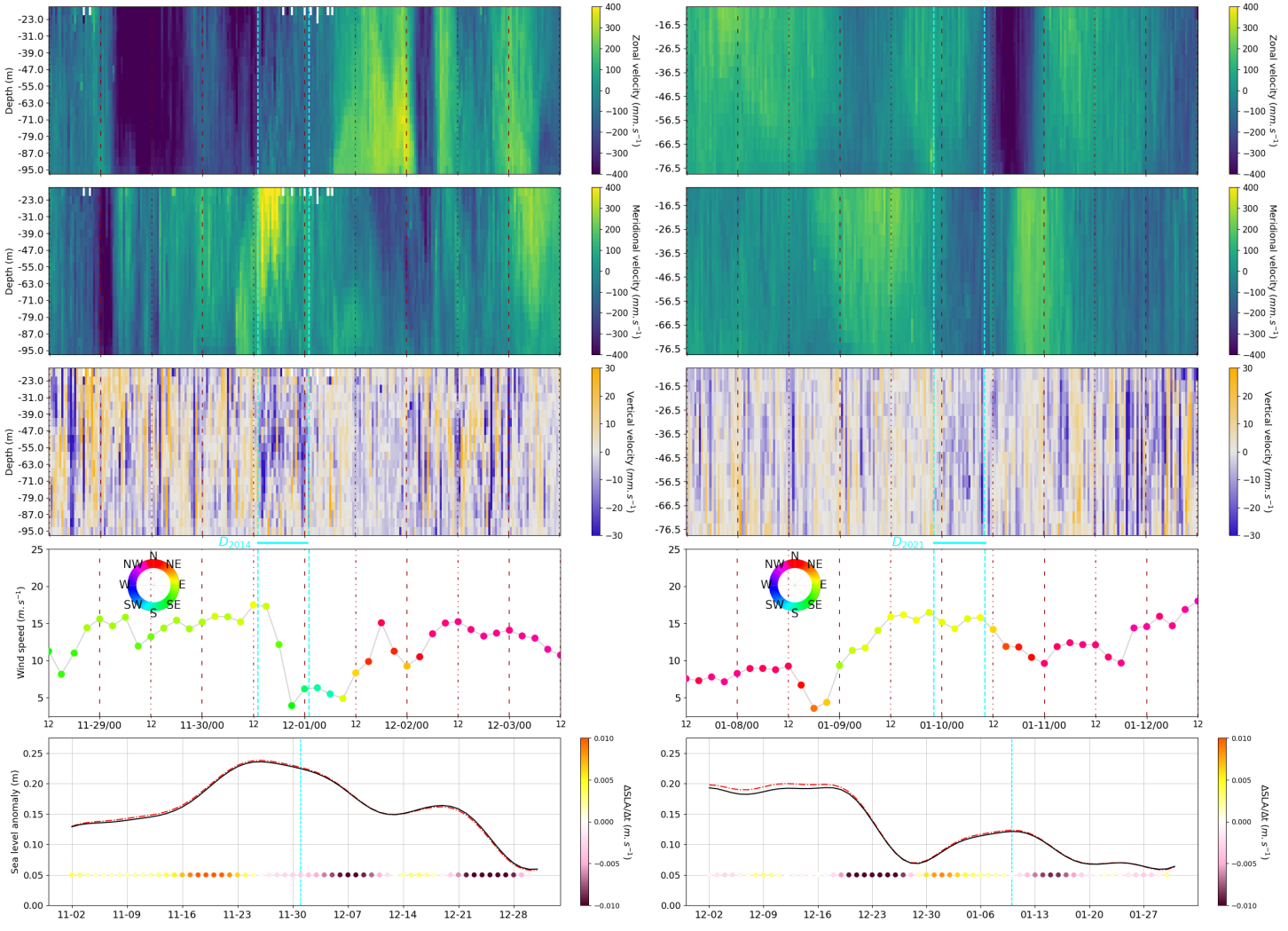

Figure 9. Top to bottom (4 panels): zonal velocity (U), meridional velocity (V), vertical velocity (W), as a function of depth and time (month-day/hour), wind intensity and direction (5 days window). Last panel: SLA observations over 2 months (month-day) at JULIO (dashed red line for JULIO nearest SLA point, solid black line for an average on $\Delta lat = 0.14$ and $\Delta lon = 0.18$ centered on this point), and SLA temporal gradient (colored dots). The left and right panels show the two different downwellings: D_{2014} (left) and D_{2021} (right), each indicated between the two vertical cyan lines.

On Figure 10, as opposed to Figure 3, the months sampled can be identified and henceforth how they were impacted by biology-induced vertical velocities. As probability density functions (PDFs) highlight a faint positive skewness in vertical velocities measured in 2013 only, the depth-time average shows that this year was sampled only from late September to the end of December, with small influence of biology-induced negative vertical velocities. Moreover, a look at wind directions and intensities during this period (data not shown) indicates that: from September to December 2013, 49.5% of wind directions

https://doi.org/10.5194/egusphere-2025-2757
Preprint. Discussion started: 8 July 2025

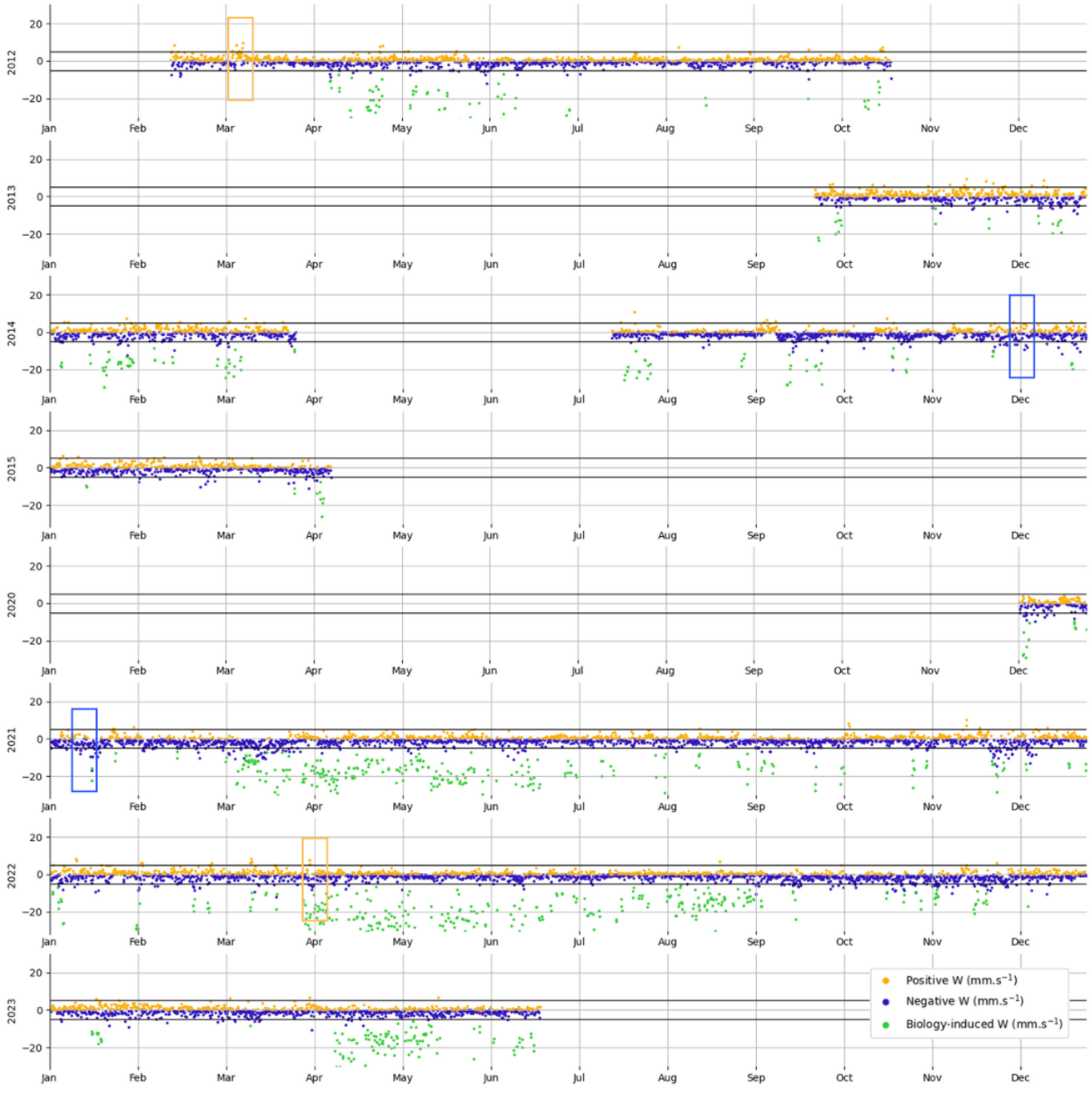

Figure 10. Depth-time average (over the whole water column, with a rolling time window of 4 hours) of W across the entire time series. The orange (blue) scatters are positive (negative) values of W, and the green scatters represent what is identified as biological-induced signal, and filtered out. The orange and blue boxes are respectively our targeted upwellings and downwellings.

https://doi.org/10.5194/egusphere-2025-2757
Preprint. Discussion started: 8 July 2025

were north-westerly winds, and that 95% of the wind peaks (above 15m.s^{-1}) were also north-westerly winds. Overall, no inter-annual variability seems to emerge. The two full-data years, namely 2021 and 2022, show very similar distributions, featuring a majority of negative vertical velocities with a negative median.

W measured with the ADCP at JULIO show a general variability of $5.0 \times 10^{-3}\ m\ s^{-1}$ around 0 (Fig. 10) with 50% of the values between -5 and $5 \times 10^{-3} m\ s^{-1}$ in Fig.3. Events showing positive or negative W intensities beyond this variability are nonetheless frequently observed. Indeed, with no temporal average, depth averaged W values (Supplementary Material) exhibits maximum values around $2.55 \times 10^{-2}\ m\ s^{-1}$ for U_{2012} and U_{2022}, versus minimum values around $-1.93 \times 10^{-2}\ m\ s^{-1}$ for D_{2014} and D_{2021}. The 4-hour depth-time averaged W (Fig. 10) exhibit maximum values of $8.5 \times 10^{-3}\ m\ s^{-1}$ (respectively $7.7 \times 10^{-3}\ m\ s^{-1}$) during U_{2012} (respectively U_{2022}). Regarding downwellings, minimum values were detected at $-6.5 \times 10^{-3}\ m\ s^{-1}$ (respectively $-5.7 \times 10^{-3}\ m\ s^{-1}$) during D_{2014} (respectively D_{2021}). On the other hand, the previously described upwelling and downwelling W (48 hours time-depth averaged for upwellings and 12 hours time-depth averaged for downwellings) logically exhibit lower intensity values with 1.0×10^{-3} and $1.6 \times 10^{-3}\ m\ s^{-1}$ for U_{2012} and U_{2022} respectively, and -5.4×10^{-3}, $-4.0 \times 10^{-3}\ m\ s^{-1}$ for D_{2014} and D_{2021} respectively. This highlights the logical link: the larger the observations time duration the smaller the averaged values, due to W variability. Indeed, upwellings present a large time-variability with the presence of both positive and negative velocities covering the entire water column, lowering their averaged time-depth values.

We have presented in this paper the first measurement of vertical velocities associated with upwelling or downwellings detected with an ADCP in the Northwestern Mediterranean Sea.

Different upwelling systems and their associated vertical velocities have been studied in other coastal environments. Estimated W from ω-equation allowed Ngo and Hsin (2024) in the Vietnamese upwelling system to reach values of the order of $10^{-1}\ m\ day^{-1}$. On the other hand, Johnson (1977) used the continuity equation to estimate W around $10^{-4}\ m\ s^{-1}$ in the Oregon upwelling system. Such values are weaker than our observations. However, Mauzole et al. (2020) obtained vertical velocities up to $20\ m\ day^{-1}$ in a coastal upwelling in the California Current System area using a general circulation model.

In our area of study, Bakun and Agostini (2001) estimated vertical velocities greater than $0.5\ m\ day^{-1}$ at the bottom of the surface Ekman layer using the continuity equation. Other upwelling cases have been studied by Berta et al. (2018), linking their occurences to strong (above $10\ m\ s^{-1}$) north-westerly wind episodes lasting 2 to 3 days which is consistent with our model outputs (Fig. 7). Using temperature and wind observations, Odic et al. (2022) observed that upwellings and downwellings exhibit a seasonality as they are less frequent during autumn and summer than during spring and winter which is consistent with our four observed events.

The durations of both upwellings in this study (Fig. 7) are similar to the observed ones in Mourre et al. (2022), who detected an upwelling in the Balearic Islands by combining model outputs and satellite observations. In terms of intensities, the latter exhibits episodic vertical velocity values between 60 and 80 $m\ day^{-1}$, which is equivalent to about 0.7×10^{-3} to $0.9 \times 10^{-3}\ m\ s^{-1}$, about half the intensity of the upwellings shown here.

Our observed upwellings show southeast horizontal currents lining up on the path of the north-westerly winds over the entire water column. Note that the classic Ekman direction of the horizontal currents is generally more visible offshore, as shown

https://doi.org/10.5194/egusphere-2025-2757
Preprint. Discussion started: 8 July 2025

in the upwelling case of Barrier et al. (2016) covering the same area. The wind intensity drives the duration of the upwelling, as intense W appear when wind intensity equals or exceeds 15 $m\ s^{-1}$, and stops as soon as the wind intensity falls below the same threshold. The two days of upwelling (U_{2022}) also affect the usual pattern of biological signal at night (Fig. 7, right W). For both upwellings, their appearance is concomitant with the strongest SST drops on a two months time window. SST observations a week before U_{2012} also exhibit the same drop, matching north-westerly wind and intense positive and negative W shifts lasting 12 hours, but not allowing an unambiguous upwelling characterization. SST satellite observations for U_{2022} were also compared to in situ surface temperature observations, highlighting negative shifts of ≈ 1°C and ≈ 2°C for satellite, and in situ observations respectively. These corresponded to the biggest temperature drops in two months for both surface observations. Despite the proximity to the coast, in situ SST observations allow to confirm satellite observations.

Both downwellings appear to happen during a SLA peak or a post peak descent (all peaks lasting several days). With shorter time window (12 hours) than upwellings (48 hours), both downwellings have averaged time-depth intensities higher than both upwellings while extreme values remain smaller than upwelling ones when no time average is applied. Indeed downwellings are more homogeneous in time than upwellings. In opposition with upwellings, they also do not always cover the entire water column. The strongest negative W are rather concentrated between 20 and 60 meters depth in our case. Easterly and south-easterly are less intense than north-westerly wind episodes. Nevertheless, the downwellings highlighted here are triggered by wind intensity values around 15 $m\ s^{-1}$ such as for upwellings. D_{2014} matches positive meridional component of current, hence onshore horizontal currents, while D_{2021} shows a strong variability in horizontal currents direction within two days. Indeed, 24 hours before D_{2021}, easterly wind matches a weak onshore current before shifting direction during D_{2021}, weakly heading offshore. Moreover, these wind episodes are notably influenced by orography, meaning that easterlies do not impact the Gulf of Lion continental shelf and offshore the same way while north-westerlies seem more homogeneous, covering the entire Gulf of Lion (see Supplementary Materials). Easterlies can as well be confined off the continental shelf with north and north-easterly winds acting as a limit and thus creating an atmospherical front. Thus, the wind measured above JULIO point may not influence directly the currents observed at JULIO, but stronger winds at higher latitudes could.

Three independent methods have been used on June 24th 2022 to measure W at JULIO (Fig. 2). After comparison, measurements show W values with intensities smaller than during the above studied dynamical events, leading to the conclusion that no upwellings or downwellings were happening on that day. Nonetheless, we observe, with the FF-ADCP, that W could vary from $-10^{-2}\ m\ s^{-1}$ to $10^{-2}\ m\ s^{-1}$ in approximately 9 min at 20 meters depth (Fig. 2), highlighting the high variability of relatively weak W. Using a meteorological model as a prediction tool could allow to set up dedicated cruises with the VVP and FF-ADCP during or right after a strong wind episode (such as Mistral or south-easterlies). They would provide W data to be compared with JULIO mooring measurements as in section 3.1, but under these different and rarely sampled circumstances.

5 Conclusions

Vertical velocities (W) are measured with the JULIO moored-ADCP, since 2012. After filtering out intense biology-induced negative W events, the remaining high-intensity W events are analyzed, with a special focus on upwellings and downwellings.

https://doi.org/10.5194/egusphere-2025-2757
Preprint. Discussion started: 8 July 2025

Two upwellings and two downwellings are thoroughly described, and show consistency between W and all the other available observations (wind model, satellite and in situ data).

This works shows that the vertical velocities can be measured with a moored-ADCP, and can be interpreted as fine-scale physical processes such as episodic coastal upwellings and downwellings in a non-rectilinear coastal site. Upwellings appear to be more easily characterized than downwellings, as they last longer, cover the entire water column and occur systematically during intense north and north-westerly winds. Downwellings occur during easterly winds and mainly in the middle of the water column, only covering ≈50 to 70% of it. Nonetheless in both upwelling and dowwelling cases, regardless of the direction, wind intensities need to be higher or on the order of $15\ m\ s^{-1}$

Such measurements exhibited strong intensity values for both upwellings and downwellings. The instantaneous maximum amplitude measured is $-1.93 \times 10^{-2}\ m\ s^{-1}$ for downwellings and $2.55 \times 10^{-2}\ m\ s^{-1}$ for upwellings. A depth-time average covering each whole event shows maximum upward W as $1.6 \times 10^{-3}\ m\ s^{-1}$ (48 hours averaged upwelling) leading to $\approx 138\ m\ day^{-1}$ and maximum amplitude for downward W as $-5.4 \times 10^{-3}\ m\ s^{-1}$ (12 hours averaged downwelling) which is equivalent to $\approx -465\ m\ day^{-1}$. The negative medians values of years 2021 and 2022 underline the potential role of biology-induced vertical velocities as these years are the only two to have been fully sampled and arise the question of 2012 where biology-induced w seem to be scarcer.

Moreover, for a first time to our knowledge, two additional in situ W measurements were performed concomitantly and their analysis shows consistency between the three type of vertical velocity measurements.

Beginning in 2025, a new-generation ADCP (Sentinel-V RDI 500kHz) with a fifth vertical acoustic beam directly measuring the vertical velocities has replaced the classical RDI OS ADCP 4-beam 300kHz at JULIO, and should provide W measurements with an increased precision.

Author contributions. MA: writing, data analysis, figures, data cleaning (JULIO 6th time serie). AP: leader of JULIO observation program, supervision, writing, data cleaning (JULIO 1st to 5th time series). JLF: scientific cruises, mooring maintenance, review, suggestions. CC: data cleaning (FF-ADCP). AB: review, suggestions. YO: provided model output data, review, suggestions. SB: supervision, writing, data cleaning (FF-ADCP & VVP). All authors contributed to the writing of the original manuscript.

Competing interests. The contact author has declared that none of the authors has any competing interests.

Acknowledgements. We adress a special thank to the MIO Physical, Littoral and Coastal Oceanography team (OPLC) for funding this work. We thank Vincent REY, Tathy MISSAMOU and Didier MALLARINO, responsible of the HTMNet (data collection and processing). We thank Anthony Bosse through the GLISS project for funding the presentation of this work at an international conference. We thank the Doctoral School of Environmental Sciences (ED251) for funding this work through the first author's PhD scholarship. We thank the captain

https://doi.org/10.5194/egusphere-2025-2757
Preprint. Discussion started: 8 July 2025

and crew of the *Antedon* research vessel. We also thank Gilles Rougier for his precious help and work on JULIO's first time series. We address a special thank to Julie Gatti who, with her pioneering PhD work, paved the way for such a study to be conducted.

https://doi.org/10.5194/egusphere-2025-2757
Preprint. Discussion started: 8 July 2025

References

Bakun, A. and Agostini, V. N.: Seasonal patterns of wind-induced upwelling/downwelling in the Mediterranean Sea, Scientia Marina, 65, 243–257, https://doi.org/10.3989/scimar.2001.65n3243, number: 3, 2001.

Barral, Q.-B.: Caractérisation du front Nord-Baléares : Variabilité et rôle de la circulation des masses d'eau en Méditerranée Occidentale, These de doctorat, Toulon, https://theses.fr/2022TOUL0006, 2022.

Barrier, N., Petrenko, A. A., and Ourmières, Y.: Strong intrusions of the Northern Mediterranean Current on the eastern Gulf of Lion: insights from in-situ observations and high resolution numerical modelling, Ocean Dynamics, 66, 313–327, https://doi.org/10.1007/s10236-016-0921-7, 2016.

Berta, M., Bellomo, L., Griffa, A., Magaldi, M. G., Molcard, A., Mantovani, C., Gasparini, G. P., Marmain, J., Vetrano, A., Béguery, L., Borghini, M., Barbin, Y., Gaggelli, J., and Quentin, C.: Wind-induced variability in the Northern Current (northwestern Mediterranean Sea) as depicted by a multi-platform observing system, Ocean Science, 14, 689–710, https://doi.org/10.5194/os-14-689-2018, 2018.

Bosse, A., Testor, P., Damien, P., Estournel, C., Marsaleix, P., Mortier, L., Prieur, L., and Taillandier, V.: Wind-Forced Submesoscale Symmetric Instability around Deep Convection in the Northwestern Mediterranean Sea, Fluids, 6, 123, https://doi.org/10.3390/fluids6030123, 2021.

Bouyssel, F., Berre, L., Bénichou, H., Chambon, P., Girardot, N., Guidard, V., Loo, C., Mahfouf, J.-F., Moll, P., Payan, C., and Raspaud, D.: The 2020 Global Operational NWP Data Assimilation System at Météo-France, in: Data Assimilation for Atmospheric, Oceanic and Hydrologic Applications (Vol. IV), edited by Park, S. K. and Xu, L., pp. 645–664, Springer International Publishing, Cham, ISBN 978-3-030-77722-7, https://doi.org/10.1007/978-3-030-77722-7_25, 2022.

Buongiorno Nardelli, B., Tronconi, C., Pisano, A., and Santoleri, R.: High and Ultra-High resolution processing of satellite Sea Surface Temperature data over Southern European Seas in the framework of MyOcean project, Remote Sensing of Environment, 129, 1–16, https://doi.org/10.1016/j.rse.2012.10.012, 2013.

Buongiorno Nardelli, B., Pisano, A., Tronconi, C., and Santoleri, R.: Evaluation of different covariance models for the operational interpolation of high resolution satellite Sea Surface Temperature data over the Mediterranean Sea, Remote Sensing of Environment, 164, 334–343, https://doi.org/10.1016/j.rse.2015.04.025, 2015.

Christensen, K. M., Gray, A. R., and Riser, S. C.: Global Estimates of Mesoscale Vertical Velocity Near 1,000 m From Argo Observations, Journal of Geophysical Research: Oceans, 129, e2023JC020 003, https://doi.org/10.1029/2023JC020003, 2024.

Cisewski, B., Hátún, H., Kristiansen, I., Hansen, B., Larsen, K. M. H., Eliasen, S. K., and Jacobsen, J. A.: Vertical Migration of Pelagic and Mesopelagic Scatterers From ADCP Backscatter Data in the Southern Norwegian Sea, Frontiers in Marine Science, 7, https://doi.org/10.3389/fmars.2020.542386, publisher: Frontiers, 2021.

Clément, L., Merckelbach, L., and Frajka-Williams, E.: Turbulent Vertical Velocities in Labrador Sea Convection, Geophysical Research Letters, 51, e2024GL110 318, https://doi.org/10.1029/2024GL110318, _eprint: https://onlinelibrary.wiley.com/doi/pdf/10.1029/2024GL110318, 2024.

Comby, C., Barrillon, S., Fuda, J.-L., Doglioli, A. M., Tzortzis, R., Grégori, G., Thyssen, M., and Petrenko, A. A.: Measuring Vertical Velocities with ADCPs in Low-Energy Ocean, Journal of Atmospheric and Oceanic Technology, 39, 1669–1684, https://doi.org/10.1175/JTECH-D-21-0180.1, 2022.

https://doi.org/10.5194/egusphere-2025-2757
Preprint. Discussion started: 8 July 2025

Cortés-Morales, D. and Lazar, A.: Vertical Velocity 3D Estimates from the Linear Vorticity Balance in the North Atlantic Ocean, Journal of Physical Oceanography, 54, 2185–2203, https://doi.org/10.1175/JPO-D-24-0011.1, publisher: American Meteorological Society Section: Journal of Physical Oceanography, 2024.

Declerck, A., Ourmières, Y., and Molcard, A.: Assessment of the coastal dynamics in a nested zoom and feedback on the boundary current: the North-Western Mediterranean Sea case, Ocean Dynamics, 66, 1529–1542, https://doi.org/10.1007/s10236-016-0985-4, 2016.

D'Asaro, E. A., Shcherbina, A. Y., Klymak, J. M., Molemaker, J., Novelli, G., Guigand, C. M., Haza, A. C., Haus, B. K., Ryan, E. H., Jacobs, G. A., Huntley, H. S., Laxague, N. J. M., Chen, S., Judt, F., McWilliams, J. C., Barkan, R., Kirwan, A. D., Poje, A. C., and Özgökmen, T. M.: Ocean convergence and the dispersion of flotsam, Proceedings of the National Academy of Sciences, 115, 1162–1167, https://doi.org/10.1073/pnas.1718453115, 2018.

d'Ovidio, F., De Monte, S., Alvain, S., Dandonneau, Y., and Lévy, M.: Fluid dynamical niches of phytoplankton types, Proceedings of the National Academy of Sciences, 107, 18 366–18 370, https://doi.org/10.1073/pnas.1004620107, publisher: Proceedings of the National Academy of Sciences, 2010.

d'Ovidio, F., Pascual, A., Wang, J., Doglioli, A. M., Jing, Z., Moreau, S., Grégori, G., Swart, S., Speich, S., Cyr, F., Legresy, B., Chao, Y., Fu, L., and Morrow, R. A.: Frontiers in Fine-Scale in situ Studies: Opportunities During the SWOT Fast Sampling Phase, Frontiers in Marine Science, 6, https://doi.org/10.3389/fmars.2019.00168, publisher: Frontiers, 2019.

Enright, J. T. and Honegger, H.-W.: Diurnal vertical migration: Adaptive significance and timing. Part 2. Test of the model: Details of timing, Limnology and Oceanography, 22, 873–886, https://doi.org/10.4319/lo.1977.22.5.0873, _eprint: https://onlinelibrary.wiley.com/doi/pdf/10.4319/lo.1977.22.5.0873, 1977.

Esposito, G., Donnet, S., Berta, M., Shcherbina, A. Y., Freilich, M., Centurioni, L., D'Asaro, E. A., Farrar, J. T., Johnston, T. M. S., Mahadevan, A., Özgökmen, T., Pascual, A., Poulain, P.-M., Ruiz, S., Tarry, D. R., and Griffa, A.: Inertial Oscillations and Frontal Processes in an Alboran Sea Jet: Effects on Divergence and Vertical Transport, Journal of Geophysical Research: Oceans, 128, e2022JC019 004, https://doi.org/10.1029/2022JC019004, _eprint: https://onlinelibrary.wiley.com/doi/pdf/10.1029/2022JC019004, 2023.

Fiekas, V., Leach, H., Mirbach, K.-J., and Woods, J. D.: Mesoscale Instability and Upwelling. Part 1: Observations at the North Atlantic Intergyre Front, Journal of Physical Oceanography, 24, 1750–1758, https://doi.org/10.1175/1520-0485(1994)024<1750:MIAUPO>2.0.CO;2, 1994.

Frajka-Williams, E., Eriksen, C. C., Rhines, P. B., and Harcourt, R. R.: Determining Vertical Water Velocities from Seaglider, Journal of Atmospheric and Oceanic Technology, 28, 1641–1656, https://doi.org/10.1175/2011JTECHO830.1, 2011.

Fuda, J.-L., Barrillon, S., Comby, C., Doglioli, A., Le Gal, P., and Petrenko, A.: Estimating ocean vertical velocities using an autonomous multipurpose profiler, in: 2023 IEEE International Workshop on Metrology for the Sea; Learning to Measure Sea Health Parameters (MetroSea), pp. 6–10, IEEE, La Valletta, Malta, ISBN 979-8-3503-4065-5, https://doi.org/10.1109/MetroSea58055.2023.10317407, 2023.

Garcia-Jove, M., Mourre, B., Zarokanellos, N. D., Lermusiaux, P. F. J., Rudnick, D. L., and Tintoré, J.: Frontal Dynamics in the Alboran Sea: 2. Processes for Vertical Velocities Development, Journal of Geophysical Research: Oceans, 127, e2021JC017 428, https://doi.org/10.1029/2021JC017428, _eprint: https://onlinelibrary.wiley.com/doi/pdf/10.1029/2021JC017428, 2022.

Gastauer, S., Nickels, C. F., and Ohman, M. D.: Body size- and season-dependent diel vertical migration of mesozooplankton resolved acoustically in the San Diego Trough, Limnology and Oceanography, 67, 300–313, https://doi.org/10.1002/lno.11993, _eprint: https://onlinelibrary.wiley.com/doi/pdf/10.1002/lno.11993, 2022.

Giordani, H., Prieur, L., and Caniaux, G.: Advanced insights into sources of vertical velocity in the ocean, Ocean Dynamics, 56, 513–524, https://doi.org/10.1007/s10236-005-0050-1, 2006.

https://doi.org/10.5194/egusphere-2025-2757
Preprint. Discussion started: 8 July 2025

Giordani, H., Lebeaupin-Brossier, C., Léger, F., and Caniaux, G.: A PV-approach for dense water formation along fronts: Application to the Northwestern Mediterranean, Journal of Geophysical Research: Oceans, 122, 995–1015, https://doi.org/10.1002/2016JC012019, _eprint: https://agupubs.onlinelibrary.wiley.com/doi/pdf/10.1002/2016JC012019, 2017.

Guenard, V., Drobinski, P., Caccia, J.-L., Campistron, B., and Bench, B.: An Observational Study of the Mesoscale Mistral Dynamics, Boundary-Layer Meteorology, 115, 263–288, https://doi.org/10.1007/s10546-004-3406-z, 2005.

Guerra, D., Schroeder, K., Borghini, M., Camatti, E., Pansera, M., Schroeder, A., Sparnocchia, S., and Chiggiato, J.: Zooplankton diel vertical migration in the Corsica Channel (north-western Mediterranean Sea) detected by a moored acoustic Doppler current profiler, Ocean Science, 15, 631–649, https://doi.org/10.5194/os-15-631-2019, 2019.

Haney, J. F.: Diel Patterns of Zooplankton Behavior, Bulletin of Marine Science, 43, 583–603, 1988.

He, J. and Mahadevan, A.: Vertical Velocity Diagnosed From Surface Data With Machine Learning, Geophysical Research Letters, 51, e2023GL104 835, https://doi.org/10.1029/2023GL104835, _eprint: https://onlinelibrary.wiley.com/doi/pdf/10.1029/2023GL104835, 2024.

Heywood, K. J.: Diel vertical migration of zooplankton in the Northeast Atlantic, Journal of Plankton Research, 18, 163–184, https://doi.org/10.1093/plankt/18.2.163, 1996.

Hoskins, B. J., Draghici, I., and Davies, H. C.: A new look at the ω-equation, Quarterly Journal of the Royal Meteorological Society, 104, 31–38, https://doi.org/10.1002/qj.49710443903, 1978.

Jakes, M., Phillips, H., Foppert, A., Cyriac, A., Bindoff, N., Rintoul, S., and Thompson, A.: Observational Evidence of Cold Filamentary Intensification in an Energetic Meander of the Antarctic Circumpolar Current, Journal of Physical Oceanography, 54, https://doi.org/10.1175/JPO-D-23-0085.1, 2024.

Johnson, D. R.: Determining vertical velocities during upwelling off the Oregon coast, Deep Sea Research, 24, 171–180, https://doi.org/10.1016/0146-6291(77)90551-3, 1977.

Lamy, A., Millot, C., and Molines, J. M.: Bottom Pressure and Sea Level Measurements in the Gulf of Lions, Journal of Physical Oceanography, 11, 394–409, https://doi.org/10.1175/1520-0485(1981)011<0394:BPASLM>2.0.CO;2, publisher: American Meteorological Society Section: Journal of Physical Oceanography, 1981.

Lebeaupin Brossier, C., Drobinski, P., Béranger, K., Bastin, S., and Orain, F.: Ocean memory effect on the dynamics of coastal heavy precipitation preceded by a mistral event in the northwestern Mediterranean, Quarterly Journal of the Royal Meteorological Society, 139, 1583–1597, https://doi.org/10.1002/qj.2049, _eprint: https://onlinelibrary.wiley.com/doi/pdf/10.1002/qj.2049, 2013.

Mahadevan, A.: The Impact of Submesoscale Physics on Primary Productivity of Plankton, Annual Review of Marine Science, 8, 161–184, https://doi.org/10.1146/annurev-marine-010814-015912, publisher: Annual Reviews, 2016.

Mahadevan, A. and Tandon, A.: An analysis of mechanisms for submesoscale vertical motion at ocean fronts, Ocean Modelling, 14, 241–256, https://doi.org/10.1016/j.ocemod.2006.05.006, 2006.

Margirier, F., Bosse, A., Testor, P., L'Hévéder, B., Mortier, L., and Smeed, D.: Characterization of Convective Plumes Associated With Oceanic Deep Convection in the Northwestern Mediterranean From High-Resolution In Situ Data Collected by Gliders, Journal of Geophysical Research: Oceans, 122, 9814–9826, https://doi.org/10.1002/2016JC012633, 2017.

Mauzole, Y. L., Torres, H. S., and Fu, L.-L.: Patterns and Dynamics of SST Fronts in the California Current System, Journal of Geophysical Research: Oceans, 125, e2019JC015 499, https://doi.org/10.1029/2019JC015499, _eprint: https://agupubs.onlinelibrary.wiley.com/doi/pdf/10.1029/2019JC015499, 2020.

https://doi.org/10.5194/egusphere-2025-2757
Preprint. Discussion started: 8 July 2025

Merckelbach, L., Smeed, D., and Griffiths, G.: Vertical Water Velocities from Underwater Gliders, Journal of Atmospheric and Oceanic Technology, 27, 547–563, https://doi.org/10.1175/2009JTECHO710.1, 2010.

Millot, C.: Circulation in the Western Mediterranean Sea, Journal of Marine Systems, 20, 423–442, https://doi.org/10.1016/S0924-7963(98)00078-5, 1999.

Millot, C. and Taupier-Letage, I.: Circulation in the Mediterranean Sea, in: The Mediterranean Sea, edited by Saliot, A., vol. The Mediterranean Sea of *Handbook of Environmental Chemistry*, pp. 29–66, Springer, https://doi.org/10.1007/b107143, 2005.

Molinari, R. and Kirwan, A. D.: Calculations of Differential Kinematic Properties from Lagrangian Observations in the Western Caribbean Sea, Journal of Physical Oceanography, 5, 483–491, https://doi.org/10.1175/1520-0485(1975)005<0483:CODKPF>2.0.CO;2, publisher: American Meteorological Society Section: Journal of Physical Oceanography, 1975.

Mourre, B., Reyes, E., Lorente, P., Novaes de Santana, A., Hernández-Lasheras, J., Hernández-Carrasco, I., Navarro, M., and Zarokanellos, N.: Intense wind-driven coastal upwelling in the Balearic Islands in response to storm Blas (November 2021), https://doi.org/10.5194/sp-2022-9, 2022.

Ngo, M.-H. and Hsin, Y.-C.: Three-dimensional structure of temperature, salinity, and Velocity of the summertime Vietnamese upwelling system in the South China Sea on the interannual timescale, Progress in Oceanography, 229, 103 354, https://doi.org/10.1016/j.pocean.2024.103354, 2024.

Odic, R., Bensoussan, N., Pinazo, C., Taupier-Letage, I., and Rossi, V.: Sporadic wind-driven upwelling/downwelling and associated cooling/warming along Northwestern Mediterranean coastlines, Continental Shelf Research, 250, 104 843, https://doi.org/10.1016/j.csr.2022.104843, 2022.

Petrenko, A., Barrier, N., Libes, M., and Quentin, C.: JULIO - Judicious Location for Intrusions Observations, https://doi.org/10.17882/91036, 2023.

Petrenko, A. A.: Variability of circulation features in the Gulf of Lion NW Mediterranean Sea. Importance of inertial currents, Oceanologica Acta, 26, 323–338, https://doi.org/10.1016/S0399-1784(03)00038-0, 2003.

Phillips, H. E. and Bindoff, N. L.: On the nonequivalent barotropic structure of the Antarctic Circumpolar Current: An observational perspective, Journal of Geophysical Research: Oceans, 119, 5221–5243, https://doi.org/10.1002/2013JC009516, _eprint: https://onlinelibrary.wiley.com/doi/pdf/10.1002/2013JC009516, 2014.

Pollard, R. T. and Regier, L. A.: Vorticity and Vertical Circulation at an Ocean Front, Journal of Physical Oceanography, 22, 609–625, https://doi.org/10.1175/1520-0485(1992)022<0609:VAVCAA>2.0.CO;2, publisher: American Meteorological Society Section: Journal of Physical Oceanography, 1992.

Ragone, F., Meli, A., Napoli, A., and Pasquero, C.: Ocean Surface Anomalies after Strong Winds in the Western Mediterranean Sea, Journal of Marine Science and Engineering, 7, 182, https://doi.org/10.3390/jmse7060182, 2019.

Rey, V., Dufresne, C., Fuda, J.-L., Mallarino, D., Missamou, T., Paugam, C., Rougier, G., and Taupier-Letage, I.: On the use of long-term observation of water level and temperature along the shore for a better understanding of the dynamics: example of Toulon area, France, Ocean Dynamics, 70, 913–933, https://doi.org/10.1007/s10236-020-01363-7, 2020.

Richez, C.: The West Spitsbergen Current as seen by SOFAR floats during the ARCTEMIZ 88 Experiment: Statistics, differential kinematic properties, and potential vorticity balance, Journal of Geophysical Research: Oceans, 103, 15 539–15 565, https://doi.org/10.1029/97JC02421, _eprint: https://onlinelibrary.wiley.com/doi/pdf/10.1029/97JC02421, 1998.

Righi, D. D. and Strub, P. T.: The use of simulated drifters to estimate vorticity, Journal of Marine Systems, 29, 125–140, https://doi.org/10.1016/S0924-7963(01)00013-6, 2001.

https://doi.org/10.5194/egusphere-2025-2757
Preprint. Discussion started: 8 July 2025

Rousselet, L., Doglioli, A. M., de Verneil, A., Pietri, A., Della Penna, A., Berline, L., Marrec, P., Grégori, G., Thyssen, M., Carlotti, F., Barrillon, S., Simon-Bot, F., Bonal, M., d'Ovidio, F., and Petrenko, A.: Vertical Motions and Their Effects on a Biogeochemical Tracer in a Cyclonic Structure Finely Observed in the Ligurian Sea, Journal of Geophysical Research: Oceans, 124, 3561–3574, https://doi.org/10.1029/2018JC014392, _eprint: https://onlinelibrary.wiley.com/doi/pdf/10.1029/2018JC014392, 2019.

Rudnick, D. L.: Intensive surveys of the Azores Front: 2. Inferring the geostrophic and vertical velocity fields, Journal of Geophysical Research: Oceans, 101, 16 291–16 303, https://doi.org/10.1029/96JC01144, 1996.

Ruiz, S., Pascual, A., Garau, B., Pujol, I., and Tintoré, J.: Vertical motion in the upper ocean from glider and altimetry data, Geophysical Research Letters, 36, https://doi.org/10.1029/2009GL038569, _eprint: https://onlinelibrary.wiley.com/doi/pdf/10.1029/2009GL038569, 2009.

Sammartino, S., García-Lafuente, J., Nadal, I., and Sánchez-Leal, R. F.: Coupled echosounder and Doppler profiler measurements in the Strait of Gibraltar, Scientific Reports, 14, 31 261, https://doi.org/10.1038/s41598-024-82670-7, publisher: Nature Publishing Group, 2024.

Siegel, D. A., DeVries, T., Cetinić, I., and Bisson, K. M.: Quantifying the Ocean's Biological Pump and Its Carbon Cycle Impacts on Global Scales, Annual Review of Marine Science, 15, 329–356, https://doi.org/10.1146/annurev-marine-040722-115226, 2023.

Soukissian, T. and Sotiriou, M.-A.: Long-Term Variability of Wind Speed and Direction in the Mediterranean Basin, Wind, 2, 513–534, https://doi.org/10.3390/wind2030028, number: 3 Publisher: Multidisciplinary Digital Publishing Institute, 2022.

Sourisseau, M., Simard, Y., and Saucier, F. J.: Krill diel vertical migration fine dynamics, nocturnal overturns, and their roles for aggregation in stratified flows, Canadian Journal of Fisheries and Aquatic Sciences, 65, 574–587, https://doi.org/10.1139/f07-179, publisher: NRC Research Press, 2008.

Spydell, M. S., Feddersen, F., and Macmahan, J.: The Effect of Drifter GPS Errors on Estimates of Submesoscale Vorticity, Journal of Atmospheric and Oceanic Technology, 36, 2101–2119, https://doi.org/10.1175/JTECH-D-19-0108.1, 2019.

Tarling, G., Thorpe, S., Fielding, S., Klevjer, T., Ryabov, A., and Somerfield, P.: Varying depth and swarm dimensions of open-ocean Antarctic krill Euphausia superba Dana, 1850 (Euphausiacea) over diel cycles, Journal of Crustacean Biology, https://doi.org/10.1093/jcbiol/ruy040, 2018.

Tarling, G. A. and Thorpe, S. E.: Oceanic swarms of Antarctic krill perform satiation sinking, Proceedings of the Royal Society B: Biological Sciences, 284, 20172 015, https://doi.org/10.1098/rspb.2017.2015, publisher: Royal Society, 2017.

Tarling, G. A., Klevjer, T., Fielding, S., Watkins, J., Atkinson, A., Murphy, E., Korb, R., Whitehouse, M., and Leaper, R.: Variability and predictability of Antarctic krill swarm structure, Deep Sea Research Part I: Oceanographic Research Papers, 56, 1994–2012, https://doi.org/10.1016/j.dsr.2009.07.004, 2009.

Tarry, D. R., Essink, S., Pascual, A., Ruiz, S., Poulain, P., Özgökmen, T., Centurioni, L. R., Farrar, J. T., Shcherbina, A., Mahadevan, A., and D'Asaro, E.: Frontal Convergence and Vertical Velocity Measured by Drifters in the Alboran Sea, Journal of Geophysical Research: Oceans, 126, e2020JC016 614, https://doi.org/10.1029/2020JC016614, 2021.

Tarry, D. R., Ruiz, S., Johnston, T. M. S., Poulain, P., Özgökmen, T., Centurioni, L. R., Berta, M., Esposito, G., Farrar, J. T., Mahadevan, A., and Pascual, A.: Drifter Observations Reveal Intense Vertical Velocity in a Surface Ocean Front, Geophysical Research Letters, 49, e2022GL098 969, https://doi.org/10.1029/2022GL098969, 2022.

Testor, P., Bosse, A., Houpert, L., Margirier, F., Mortier, L., Legoff, H., Dausse, D., Labaste, M., Karstensen, J., Hayes, D., Olita, A., Ribotti, A., Schroeder, K., Chiggiato, J., Onken, R., Heslop, E., Mourre, B., D'ortenzio, F., Mayot, N., Lavigne, H., de Fommervault, O., Coppola, L., Prieur, L., Taillandier, V., Durrieu de Madron, X., Bourrin, F., Many, G., Damien, P., Estournel, C., Marsaleix, P., Taupier-Letage, I., Raimbault, P., Waldman, R., Bouin, M.-N., Giordani, H., Caniaux, G., Somot, S., Ducrocq, V.,

https://doi.org/10.5194/egusphere-2025-2757
Preprint. Discussion started: 8 July 2025

and Conan, P.: Multiscale Observations of Deep Convection in the Northwestern Mediterranean Sea During Winter 2012–2013 Using Multiple Platforms, Journal of Geophysical Research: Oceans, 123, 1745–1776, https://doi.org/10.1002/2016JC012671, _eprint: https://onlinelibrary.wiley.com/doi/pdf/10.1002/2016JC012671, 2018.

Thurnherr, A. M.: Vertical velocity from LADCP data, in: 2011 IEEE/OES 10th Current, Waves and Turbulence Measurements (CWTM), pp. 198–204, IEEE, Monterey, CA, USA, ISBN 978-1-4244-9285-5, https://doi.org/10.1109/CWTM.2011.5759552, 2011.

Tintoré, J., Gomis, D., Alonso, S., and Parrilla, G.: Mesoscale Dynamics and Vertical Motion in the Alborán Sea, Journal of Physical Oceanography, 21, 811–823, https://doi.org/10.1175/1520-0485(1991)021<0811:MDAVMI>2.0.CO;2, publisher: American Meteorological Society Section: Journal of Physical Oceanography, 1991.

Tzortzis, R., Doglioli, A. M., Barrillon, S., Petrenko, A. A., d'Ovidio, F., Izard, L., Thyssen, M., Pascual, A., Barceló-Llull, B., Cyr, F., Tedetti, M., Bhairy, N., Garreau, P., Dumas, F., and Gregori, G.: Impact of moderately energetic fine-scale dynamics on the phytoplankton community structure in the western Mediterranean Sea, Biogeosciences, 18, 6455–6477, https://doi.org/10.5194/bg-18-6455-2021, publisher: Copernicus GmbH, 2021.

van Haren, H.: Internal wave–zooplankton interactions in the Alboran Sea (W-Mediterranean), Journal of Plankton Research, 36, 1124–1134, https://doi.org/10.1093/plankt/fbu031, 2014.

Zhu, R., Yang, H., Li, M., Chen, Z., Ma, X., Cai, J., and Wu, L.: Observations reveal vertical transport induced by submesoscale front, Scientific Reports, 14, 4407, https://doi.org/10.1038/s41598-024-54940-x, publisher: Nature Publishing Group, 2024.